Micro-transfer-printed Membrane DR Lasers on Si Waveguide Modulated with 50-Gbit/s NRZ Signal

Yoshiho Maeda [(1)], Takuro Fujii[(1)], Takuma Aihara[(1)], Tatsurou Hiraki[(1)], Koji Takeda[(1)], Tai Tsuchizawa[(1)], Hiroki Sugiyama[(1)], Tomonari Sato[(1)], Toru Segawa[(1)], Yasutomo Ota[(2,3)], Satoshi Iwamoto[(2,4)], Yasuhiko Arakawa[(2)], and Shinji Matsuo[(1)]

[(1)] NTT Device Technology Labs, NTT Corporation, 3-1 Morinosato Wakamiya, Atsugi-shi, Kanagawa 243-0198, Japan, yoshiho.maeda.gk@hco.ntt.co.jp
[(2)] Institute for Nano Quantum Information Electronics, The University of Tokyo, 4-6-1 Komaba, Meguro-ku, Tokyo 153-8505, Japan
[(3)] Department of Applied Physics and Physico-Informatics, Keio University, 3-14-1 Hiyoshi, Kohoku-ku, Yokohama-shi, Kanagawa 223-8522, Japan
[(4)] Institute of Industrial Science, The University of Tokyo, 4-6-1 Komaba, Meguro-ku, Tokyo 153-8505, Japan

Abstract *We fabricate directly modulated membrane distributed reflector lasers on a Si waveguide by using the micro-transfer printing. A low threshold current of 1.2 mA and good optical coupling between the laser output and 220-nm-thick Si waveguides are achieved. 50-Gbit/s NRZ signal modulation is also demonstrated. ©2022 The Author(s)*

Introduction

Co-packaged optics (CPO) is attracting attention as a way to overcome the bandwidth and power consumption limitations of electrical inputs and outputs [1]. Photonic integrated circuits (PICs) based on silicon photonics (SiPh) enable CPO to outperform electrical connections, such as a peripheral component interconnect express (PCIe), because they can be used to make compact and high-performance Si waveguide circuits on silicon-on-insulator (SOI) wafers [2-3].

High-density integration of III-V light sources and other optoelectronic components is a critical issue on this platform. Here, micro-transfer printing, which combines the flexibility of hybrid integration with high throughput, is a promising way to integrate various III-V devices on SiPh PICs [4-13]. Although high alignment accuracy has been demonstrated, a complicated III-V device structure using multiple steps of etching is required to obtain a good optical coupling between the III-V and Si waveguides [13].

We have developed membrane lasers and other optical components that use a thin III-V layer with a lateral *p-i-n* junction [14-20]. This structure enables us to achieve a large optical confinement of the active region and provides high-modulation efficiency with low power consumption [16]. Another important feature of the membrane III-V device is that the thickness and refractive index are close to those of the Si waveguide, so that a good optical coupling can be achieved with a simple taper structure [20]. This structure is quite suitable for transfer printing.

In this work, we fabricated membrane directly modulated lasers (DMLs) on Si waveguides (SOI substrate) by utilizing the micro-transfer printing and investigated their lasing properties for the first time. The lasers had a low threshold current of 1.2 mA. Furthermore, we achieved a good optical coupling between the III-V and 220-nm-thick Si waveguides and single mode operation in the C-band. We also examined the eye-opening of 50-Gbit/s NRZ signals.

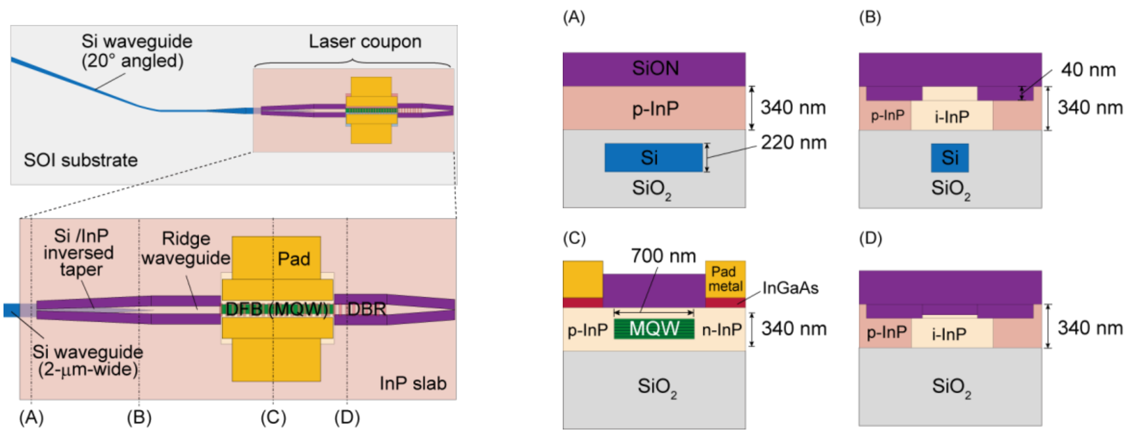

Fig. 1: Schematic diagram and cross-sections of the transfer-printed membrane DR laser on Si waveguide (SOI substrate).

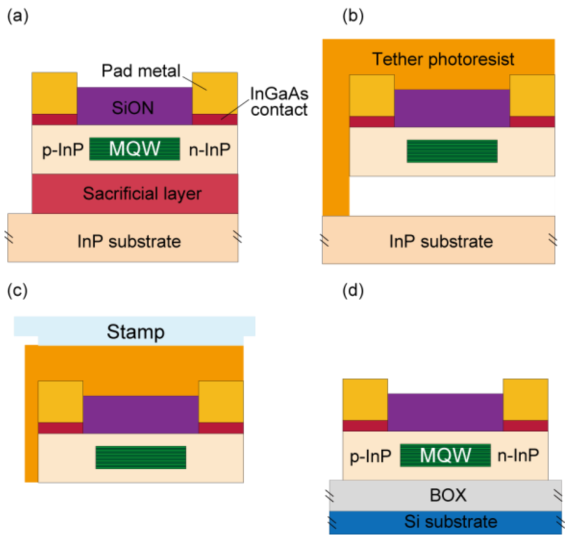

Fig. 2: Procedure for fabricating membrane lasers on Si waveguide by micro-transfer printing.

Device structure and fabrication process

Figure 1 shows schematic diagram and cross-sections of the device, in which a membrane distributed-reflector (DR) laser is transfer-printed on a Si waveguide. The dimensions of the laser coupon were 160 × 700 μm^2, which is enough area for fabricating large pad electrodes and a long InP taper waveguide. We designed a DR laser consisting of a 140-μm-long distributed feedback (DFB) active section and a 60-μm-long distributed Bragg reflector (DBR). We used a uniform DFB and DBR grating, whose coupling coefficients were 550 cm^{-1} for the DFB region and 250 cm^{-1} for the DBR region. Single-mode lasing was achieved with the DBR in order to select one of the DFB sidebands. For an efficient optical coupling between the Si and laser output waveguides, it is important to design a coupler that takes into account the misalignment of transfer printing. We designed 100-μm-long InP/Si inverse tapers with a shallow (~ 40-nm-depth) ridge-type InP waveguide for mode transfer (cross-sections (A) and (B)). The inter-layer of SiO_2 between laser coupon and Si waveguide was 100-nm thick for efficient optical mode coupling. Si waveguide was angled at 20° toward the chip facet and widened to a 5 μm in order to suppress reflections at the chip facet. In addition, the width of the Si waveguide at the laser coupon edge was widened to 2 μm, where the optical mode is mainly confined within the wide Si waveguide, which results in reduced reflection at the coupon edge. As shown in cross-section (C) in Fig. 1, there is no Si waveguide underneath the active region, which enables us to achieve a large optical confinement factor.

To fabricate laser coupons, six InGaAsP-based MQWs and a 500-nm thick InAlAs

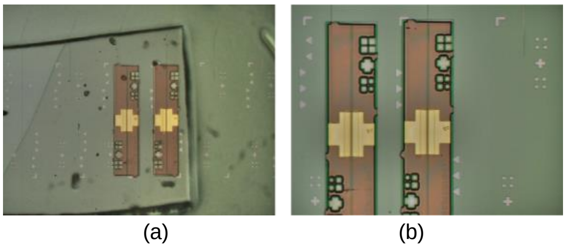

Fig. 3: Optical microscope image of laser coupons in the micro-transfer-printing process.

sacrificial layer were grown on InP substrate. After fabricating the buried active region, a lateral *p-i-n* structure was formed using the selective doping technique. We used a buried InP layer for forming the front and rear ridge waveguides. Then, the grating section, InGaAs contact layer, and pad electrodes were fabricated.

Figure 2(a)-(d) illustrates the micro-transfer printing method. As shown in Fig. 2(a), a SiON cover layer was deposited to protect the InGaAs contact layer during the sacrificial layer etching process. The coupons were covered with photoresist, with local openings to access the sacrificial layer. The sacrificial layer was then selectively etched, leaving the devices or material coupons attached to the substrate by photoresist tether structures (Fig. 2(b)). After that, these coupons were picked up from the InP substrate by breaking the tether structures using a polydimethylsiloxane (PDMS) stamp (Fig. 2(c)). Finally, the coupons were printed on the Si waveguide of the target wafer with high accuracy alignment (Fig. 2(d)). Fig. 3(a) and (b) are top-view images of the coupons after pick-up and the printed coupons. The highly transparent PDMS stamp enabled the coupon to be accurately aligned with the alignment marks on the SOI substrate by using a high-resolution visible camera and microscope.

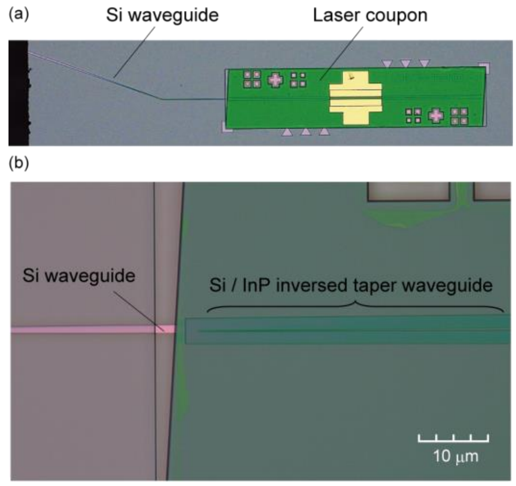

Fig. 4: (a) Optical microscope image of transfer-printed laser coupon on Si waveguide chip (SOI substrate) and (b) zoomed image of Si/InP inversed taper waveguide region near the laser coupon edge.

Results and discussion

Figure 4(a) and (b) show a transferred laser coupon. The misalignment was several hundred nm parallel and perpendicular to the direction of light propagation

Figure 5 shows the output light versus bias current (*L-I* curve) and the voltage versus bias current (*V-I* curve). The maximum optical power received by the large-area photodetector (PD) was about 0.8 mW. The threshold current was 1.2 mA, which is similar to the value of our previous device fabricated with a wafer-scale process [13-15]. The kink in the *L-I* curve is due to the reflection at the chip facet as described below.

Figure 6 (a) shows the lasing spectra at 25°C, where the bias current was varied from 2 to 14 mA. Single mode operation and side mode suppression ratios (SMSR) of up to 40 dB were realized. As shown in Fig. 6 (b), some optical reflection from the laser coupon edge and Si waveguide chip facet remains. However, the main cause of the ripples (its free spectral range (FSR) is about 0.35 nm) in the spectrum (Fig. 6 (inset)) is the reflection at the chip facet. This indicates that the optical mode field at the InP coupon edge is mainly confined in the 2-μm-wide-Si waveguide and the reflection at the coupon edge is sufficiently suppressed. The reflections at the fibre and Si waveguide can be suppressed by integrating a SiO_x spot-size-converter [20].

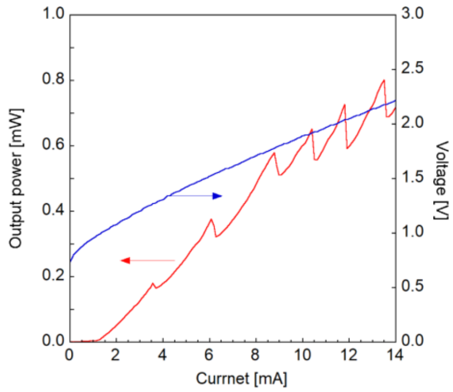

Fig. 5: Measured *L-I* (red) and *V-I* (blue) curves.

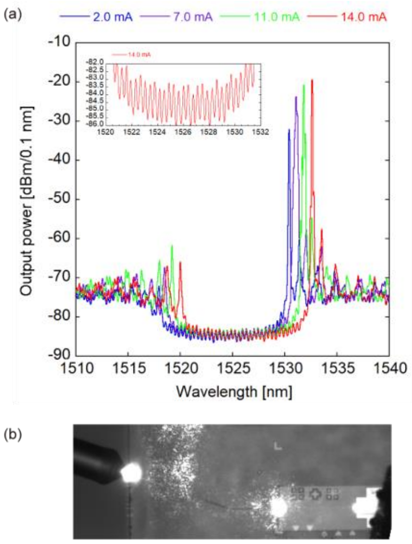

Fig. 6: (a) Lasing spectra at 25°C, where the bias current is 2-14 mA, (inset) spectrum ripples in DFB stopband and (b) IR camera image at a bias current of 10 mA.

Figure 7 (a), and (b) shows the measured eye diagram of the 40- and 50-Gbit/s NRZ signals for a 2^{31}-1 pseudo-random bit sequence (PRBS). The NRZ signals were generated by a pulse pattern generator (PPG), and a 4ch-MUX (Anritsu, MU183021A) was used to obtain the input peak-to-peak voltages of 0.7-0.8 V_{pp}. The DML was driven by a 65-GHz bias tee and a 67-GHz RF probe. In order to acquire the eye diagrams with digital communication analyzers (Keysight, N1000A), the optical power coupled to a lensed fibre was amplified with an erbium-doped fibre amplifier (EDFA) and detected with an O/E converter (HP, 83440D). Eye-opening was confirmed for both data rates. The energy costs for the 40- and 50-Gbit/s NRZ signals were 0.78 pJ/bit and 0.63 pJ/bit, respectively.

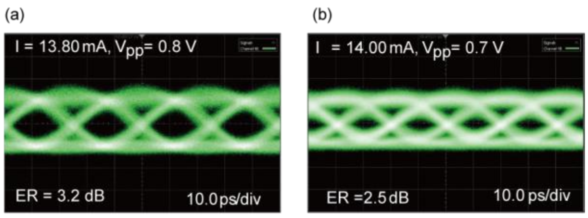

Fig. 7: (a) 40-Gbit/s and (b) 50-Gbit/s NRZ eye diagrams.

Conclusions

We investigated the characteristics of membrane DMLs on Si waveguides fabricated by micro-transfer printing. We achieved a low threshold current of 1.2 mA, maximum output power of 0.8 mW (with a PD), and single mode operation (SMSR ~ 40 dB). We also confirmed eye-opening of 40- and 50-Gbit/s NRZ signals at 25°C. Such a DML is promising for high-density integration of membrane DMLs and SiPh PICs.

Acknowledgements

We wish to thank Y. Shoji, Y. Yokoyama, Y. Ote, J. Asaoka, and S. Hirata for their support with the device fabrication and measurement.

References

[1] R. Mahajan, X. Li, J. Fryman, Z. Zhang, Nekkanty, P. Tadayon, J. Jaussi, S. Shumarayev, A. Agrawal, S. Jadhav, K. A. Singh, A. Alduino, S. Gujjula, C.-P. Chiu, T. Nordstog, K. J. Hosseini, S. Sane, N. Deshpande, K. Aygün, A. Sarkar, P. Dobriyal, S. Pothukuchi, and V. A. Pogue, and D. Hui, "Co-Packaged Photonics For High Performance Computing: Status, Challenges And Opportunities," *Journal of Lightwave Technology*, vol. 40, no. 2, pp. 379-392, 15, 2022, DOI: 10.1109/JLT.2021.3104725

[2] E. Timurdogan, Z. Su, R. Shiue, M. J. Byrd, C. V. Poulton, K. Jabon, C. DeRose, B. R. Moss, E. S. Hosseini, I. Duzevik, M. Whitson, R. P. Millman, D. A. Atlas, and M. R. Watts, "400G Silicon Photonics Integrated Circuit Transceiver Chipsets for CPO, OBO, and Pluggable Modules," in *Proceedings Optical Fiber Communication Conference (OFC) 2020*, paper T3H.2. https://ieeexplore.ieee.org/document/9083213

[3] M. Vallo and P. Mukish, "Global insights into the co-packaged technology platforms enabling transceivers with capacities of 1.6 Tbps and higher," in *Proceedings SPIE 12027, Metro and Data Center Optical Networks and Short-Reach Links V*, 120270R., 2022, DOI: 10.1117/12.2608690

[4] B. Corbett, R. Loi, W. Zhou, D. Liu, and Z. Ma, "Transfer print techniques for heterogeneous integration of photonic components," *Progress in Quantum Electronics*, vol. 52, pp. 1–17, 2017, DOI: 10.1016/j.pquantelec.2017.01.001.

[5] Z. Wang, A. Abbasi, U. Dave, A. De Groote, S. Kumari, B. Kunert, C. Merckling, M. Pantouvaki, Y. Shi, B. Tian, K. Van Gasse, J. Verbist, R. Wang, W. Xie, J. Zhang, Y. Zhu, J. Bauwelinck, X. Yin, Z. Hens, J. V. Campenhout, B. Kuyken, R. Baets, G. Morthier, D. V. Thourhout, and G. Roelkens, "Novel Light Source Integration Approaches for Silicon Photonics," *Laser & Photonics Reviews*, 11: 1700063., 2017, DOI: 10.1002/lpor.201700063

[6] H. Yang, D. Zhao, S. Chuwongin, J.-H. Seo, W. Yang, Y. Shuai, J. Berggren, M. Hammar, Z. Ma, and W. Zhou, "Transfer-printed stacked nanomembrane lasers on silicon," *Nature Photonics,* 6, 615–622, 2012, DOI: 10.1038/nphoton.2012.160

[7] J. Justice, C. Bower, M. Meitl, M. B. Mooney, M. A. Gubbins, and B. Corbett, "Wafer-scale integration of group III–V lasers on silicon using transfer printing of epitaxial layers," *Nature Photonics,* 6, 610–614, 2012, DOI: 10.1038/nphoton.2012.204

[8] A. D. Groote, P. Cardile, A. Z. Subramanian, A. M. Fecioru, C. Bower, D. Delbeke, R. Baets, and G. Roelkens, "Transfer-printing-based integration of single-mode waveguide-coupled III-V-on-silicon broadband light emitters," *Optics Express,* vol. 24, pp. 13754–13762, 2016, DOI: 10.1364/OE.24.013754

[9] J. Zhang, B. Haq, J. O'Callaghan, A. Gocalinska, E. Pelucchi, A. J. Trindade, B. Corbett, G. Morthier, and G. Roelkens, "Transfer-printing-based integration of a III-V-on-silicon distributed feedback laser," *Optics Express* vol. 26, pp. 8821-8830, 2018, DOI: 10.1364/OE.26.008821

[10] R. Katsumi, Y. Ota, M. Kakuda, S. Iwamoto, and Y. Arakawa, "Transfer-printed single-photon sources coupled to wire waveguides," *Optica,* vol. 5, pp. 691-694, 2018, DOI: 10.1364/OPTICA.5.000691

[11] R. Katsumi, Y. Ota, A. Osada, T. Tajiri, T. Yamaguchi, M. Kakuda, and Y. Arakawa, "In situ wavelength tuning of quantum-dot single-photon sources integrated on a CMOS-processed silicon waveguide," *Applied Physics Letters*, vol. 116, pp. 041103, 2020, DOI: 10.1063/1.5129325

[12] J. Zhang, E. Soltanian, B. Haq, S. Ertl,J. Rimböck, B. Matuskova, and G. Roelkens, "Integrated optical transmitter with micro-transfer-printed widely tunable III-V-on-Si laser," in *Proceedings 2022 Optical Fiber Communications Conference and Exhibition (OFC),* 2022, pp. 1-3. https://ieeexplore.ieee.org/xpl/conhome/9748173/proceeding

[13] B. Haq, S. Kumari, K. V. Gasse, J. Zhang, A. Gocalinska, E. Pelucchi, and G. Roelkens, "Micro-transfer-printed III-V on silicon C-band semiconductor optical amplifiers," *Laser & Photonics Reviews*, vol. 14, pp. 1900364, 2020, DOI: 10.1002/lpor.201900364

[14] S. Matsuo, T. Fujii, K. Hasebe, K. Takeda, T. Sato, and T. Kakitsuka, "Directly modulated buried heterostructure DFB laser on SiO2/Si substrate fabricated by regrowth of InP using bonded active layer," *Optics Express,* vol. 22, pp. 12139, 2014, DOI: 10.1364/OE.22.012139

[15] T. Fujii, K. Takeda, E. Kanno, K. Hasebe, H. Nishi, T. Yamamoto, and S. Matsuo, "Heterogeneously integrated lasers using epitaxially grown III-V active layer on directly bonded InP/SiO2/Si substrate," in *Proceedings 2016 IEEE Photonics Conference (IPC),* 2016, pp. 540-541, DOI: 10.1109/IPCon.2016.7831220

[16] T. Fujii, K. Takeda, N. P. Diamantopoulos, E. Kanno, K. Hasebe, H. Nishi, and S. Matsuo, "Heterogeneously integrated membrane lasers on Si substrate for low operating energy optical links," *Journal of Selected Topics in Quantum Electronics*, vol. 24, no. 1, pp. 1-8, 2018, DOI: 10.1109/JSTQE.2017.2778510

[17] T. Aihara, T. Hiraki, Y. Maeda, T. Fujii, T. Tsuchizawa, K. Takahata, T. Kakitsuka, and S. Matsuo, "60-GHz-bandwidth O-band Membrane InGaAlAs Electro-Absorption Modulator on Si Platform," in *Proceedings 2021 IEEE 17th International Conference on Group IV Photonics (GFP),* 2021, pp. 1-2, DOI: 10.1109/GFP51802.2021.9674001

[18] T. Hiraki, T. Aihara, Y. Maeda, T. Fujii, T. Sato, T. Tsuchizawa, S. Matsuo, K. Takahata, and T. Kakitsuka, "Over-67-GHz-bandwidth Membrane InGaAlAs EADFB Laser on Si Platform," in *Proceedings 2022 Optical Fiber Communications Conference and Exhibition (OFC),* pp. 1-3. https://ieeexplore.ieee.org/xpl/conhome/9748173/proceeding

[19] T. Hiraki, T. Aihara, Y. Maeda, T. Fujii, T. Tsuchizawa, K. Takahata, T. Kakitsuka, and S. Matsuo, "50-GHz-Bandwidth Membrane InGaAsP Electro-Absorption Modulator on Si Platform," *Journal of Lightwave Technology*, vol. 39, no. 16, pp. 5300-5306, 2021, DOI: 10.1109/JLT.2021.3082710

[20] T. Aihara, T. Hiraki, K. Takeda, T. Fujii, T. Kakitsuka, T. Tsuchizawa, and S. Matsuo, "Membrane buried-heterostructure DFB laser with an optically coupled III-V/Si waveguide," *Optics Express*, vol. 27, no. 25, pp. 36438-36448, 2019, DOI: 10.1364/OE.27.036438